PNAS RESEARCH ARTICLE | MICROBIOLOGY OPEN ACCESS

A fully synthetic Golden Gate assembly system for engineering a *Pseudomonas aeruginosa* phiKMV-like phage

Andrew P. Sikkema[a,1], Kaitlyn E. Kortright[b,c,1], Hemaa Selvakumar[d,2], Jyot Antani[b,c], Benjamin K. Chan[b,c], Matthew Davidson[b,c], Max Hopkins[d], Benjamin Newman[a], Vladimir Potapov[a], Cecilia A. Silva-Valenzuela[a], S. Kasra Tabatabaei[a], Robert McBride[d], Paul E. Turner[b,c,e,3], and Gregory J. S. Lohman[a,3]

Affiliations are included on p. 10.

Contributed by Paul E. Turner; received September 19, 2025; accepted December 17, 2025; reviewed by Jeffrey E. Barrick and Timothy K. Lu

Bacteriophages have applications in biotechnology, including human and veterinary medicine, agriculture, food safety, and biosecurity. One example of resurging importance is phage therapy, the use of phages to treat antibiotic-resistant bacterial infections. Phage therapy currently requires screening of environmental phages against the infecting strains for each individual patient, a laborious process that limits the development of standardized treatments. To overcome limitations of narrow host range inherent to many native phages, a robust genomic engineering platform is required which permits rapid and dependable genome production and engineering for nonmodel phage. Here, we describe an engineering platform for a phiKMV-like *Pseudomonas aeruginosa* phage, 41S1 that builds on previous work in the rapid assembly of small genomes through one-pot, High Complexity Golden Gate assembly (HC-GGA). This system divides the 41S1 genome into DNA fragments small enough to be conveniently synthesized and to avoid toxicity during DNA propagation, with all but one maintained in *Escherichia coli*. These fragments are readily assembled in a high accuracy, one-pot reaction; phages can be rescued by direct transformation into *P. aeruginosa* PAO1 or *E. coli* 10-beta cells. We demonstrate the precise generation of point mutations, DNA insertions, deletions, and the addition of fluorescence reporter genes that are expressed during phage replication. All viable genotypes could be generated with near 100% success rate with minimal screening. This system demonstrates the potential of HC-GGA for the rapid production and engineering of phages and provides a chassis for the development of phages that broadly target the opportunistic human pathogen *P. aeruginosa*.

bacteriophage | biotechnology | phage therapy | recombinant genetics | synthetic biology

Significance

Bacteriophages present powerful tools for combatting antibiotic-resistant bacterial infections. However evolution of bacterial resistance, narrow host range, and limited phage strain availability present challenges to the widespread use of phage therapy. The ability to engineer existing phages or synthetize strains lacking an extant sample provides a means to greatly expand the available diversity of phage strains. Here, we demonstrate the assembly and rescue of a phiKMV-like *Pseudomonas aeruginosa* bacteriophage using High-Complexity Golden Gate assembly (HC-GGA) from synthetic fragments. We subsequently precisely engineered the phage genome with modifications ranging from point mutations to gene insertions and replacements. This approach enables the construction of diverse genome modifications within phages which can further both study of their biology and increase their therapeutic potential.

The use of bacteria-specific viruses (bacteriophages, phages) in biotechnology offers the potential to address a myriad of problems in medicine, agriculture, and food safety and security (1–5). Phage therapy, the use of phages to target human pathogens, is a potential answer to the global rise in antibiotic resistant bacteria. Current implementations of this resurgent technology rely on phages isolated from the environment that can infect and kill bacterial strains otherwise resistant to traditional antibiotics. One of the often-repeated advantages of phage biotechnology is the immense repertoire of viruses that can be accessed, e.g., it is often cited that roughly 10^{32} phages exist on the planet, a number exceeding the stars in the universe (6). However, phage researchers have only isolated a few thousand phage strains, with most of those being from similar environmental sources and thus with constrained genetic diversity (7). This limited library of available phage strains must be screened against patient-specific infecting pathogens individually that typically have a large natural variance in susceptibility to phage isolates. Multiple phage strains are typically combined in a "phage cocktail" to ensure therapeutically useful coverage and to avoid the emergence of bacterial resistance to the phages used (8). To overcome issues of limited strain diversity, the slow process of screening natural isolates, and potential of narrow bacterial susceptibility, novel approaches to access a greater fraction of phage diversity, such as methods that enable reliable, high-throughput phage genomic manipulation are needed.

Engineering of lytic phages has been limited by the availability of selection tools and method dependence on multiple low-frequency events (2, 4, 9–11). Homologous recombination-based methods involve the exchange of genetic material between two phages or a phage and plasmid/retron; however, recombination frequencies are often low (10^{-4} to 10^{-10}) and require incorporation of marker genes or counterselection tools to select mutants. While recombineering methods improve the efficiency of homologous recombination significantly to ~10% positive plaques, they require a multitude of proteins

[1]A.P.S. and K.E.K. contributed equally to this work.

[2]Present address: Biopreparedness Research Virtual Environment Phage Foundry, Lawrence Berkeley National Laboratory, Berkeley, CA 94720.

[3]To whom correspondence may be addressed. Email: paul.turner@yale.edu and lohman@neb.com.

This article contains supporting information online at https://www.pnas.org/lookup/suppl/doi:10.1073/pnas.2525963123/-/DCSupplemental.

Published January 23, 2026.

including some that are specific to the bacterial species of interest. Thus, optimization of recombineering protocols is often tedious and must be redeveloped for each microbial host. More recently, CRISPR-Cas systems have been used for counterselecting recombinant phages (12, 13). This approach involves the loss of a protospacer sequence or gaining an anti-CRISPR gene by the recombinants, allowing them to thrive in counterselection strains containing CRISPR-Cas defense systems. Although counterselection helps in selecting mutant phages over wild type, other limitations emerge including enrichment of CRISPR-Cas escape mutants and the need to customize the counterselection for each mutation. Because these methods require propagation of phages, isolation of plaques, and sequencing to identify incorporation of the desired mutations, they offer little ability to generate phages purely from metagenomic datasets via synthetic DNA alone and are typically limited to altering only one genomic region at a time.

Synthetic methods of phage genome assembly have a number of advantages over in vivo recombination approaches (2, 10, 14, 15). De novo assembly of phage genomic DNA can permit rescue of viable phage particles from standard bacterial strains without complex host engineering. Further, with the ever-improving availability of synthetic DNA, access to phage isolates is not even required if complete sequence data exist. Assembly of fully synthetic phage and viral genomes has been accomplished through in vivo assembly of fragments in a secondary organism, e.g. yeast assembly in *Saccharomyces cerevisiae* in the form of a YAC containing the complete phage genome (10, 16, 17). However, passage of complete genomes through a secondary organism can be a multiday time investment, and can fall prey to mutagenesis by the carrier organism as a means of combating DNA toxicity and alterations to repeats or other genetically unstable regions (18, 19).

Recently, several labs have shown that assembly of full-length phage and viral genomes can be accomplished in one step from DNA fragments generated via PCR from genomic DNA and/or synthetic fragments (2, 10, 15, 20–24). Golden Gate assembly (GGA) has been demonstrated to allow dozens of fragments in a single reaction to assembly with high accuracy and efficiency when using comprehensive assembly fidelity data to guide junction selection (25, 26). GGA also tolerates sequence repeats and high GC content, which could be critical for successful assembly of many phage genomes. High Complexity Golden Gate assembly (HC-GGA) has been demonstrated to allow the successful assembly of *Escherichia coli* T7 phage and the *Mycobacterium smegmatis* phages BPs and Bxb1 genomes from 12 or more individual fragments in a single step (23, 25, 27). Genomes of up to 50 kb can be broken down into sequences short enough to be conveniently ordered from DNA vendors. Further, this work demonstrated that the resultant assembly products can be directly transformed into the host without cleanup, amplification, or sequence verification prior to introduction to the host, with a near 100% success rate in the introduction of the desired changes without need for a selectable marker.

Here, we extend this methodology to report a fully synthetic phiKMV-like (*Phikmvvirus* genus) phage engineering system. Phage 41S1 is a podovirus of the T7 phage superfamily with a 43 kb genome and GC content of 62% and 87% identity to phiKMV type strain (GenBank: AJ505558.1) (28), a phage that has demonstrated therapeutic potential in phage therapy (29–32). 41S1 phage targets *Pseudomonas aeruginosa*, one of the opportunistic human ESKAPE pathogens, an extraordinarily important group of microbes that are responsible for most nosocomial infections and represent paradigms of pathogenesis, transmission, and resistance (33–35). The assembly system reported here allows the assembly of the complete 41S1 genome via HC-GGA from 28 fragments, of which 27 are cloned into *E. coli* high-copy number plasmids (Fig. 1). The assembled genome can be directly transformed into the *P. aeruginosa* PAO1 strain to rescue active phages or transformed into electrocompetent *E. coli* as a surrogate host to propagate the phage. We demonstrate the ease of use of this assembly system to introduce specific mutations by modification of the fragment plasmids via classic site-directed mutagenesis (SDM) methods, resulting in recombinant phage with a very low error rate (<1 SNP per 70 kb). We altered the host range of 41S1 by swapping putative tail fiber genes from 41S1 with orthogonal genes from a related phage. We further test the tolerance of the phage for insertion of additional DNA sequences, showing that at least 1.5 kb can be stably inserted into the phage genome. Finally, we demonstrate the addition of functional payloads, adding a fluorescence reporter gene in the early genes (replacing the nonsense mutation-containing *gp6*) and one in the late genes (after the capsid protein *gp32*) in a single phage, and generation of a second phage that has a fusion of GFP to the capsid. We report details of this system and propose its use for the rapid engineering of phages to enable biological study of phage infection, and as a tool for the generation of novel phages for treatment of *P. aeruginosa* infections.

Results and Discussion

Design of 41S1 Assembly System and Golden Gate Assembly. 41S1 is a phiKMV-like phage isolated from sewage sample collected from New Haven, CT, in 2016 and isolated by established methods (36). Fig. 1 displays a schematic of the 41S1 genome highlighting annotated ORFs and selected fragment fusion sites. Based on our prior results, where a circular form construct improves successful transformation and rescue of *E. coli* T7 phage, a similar circular assembly approach was used here (23). The 41S1 genome was analyzed for internal Type IIS recognition sites for common GGA Type IIS enzymes, and BsmBI was chosen for having the fewest number of native sites to be eliminated. Native BsmBI sites in intragenic regions were removed by silent mutations following a codon usage table for *P. aeruginosa* PAO1 (37). BsmBI sites in intergenic regions were removed by comparison to other *Phikmvvirus* sequences, modifying them to conserved sequences that lack BsmBI sites (*SI Appendix*, Table S1 and Fig. S1).

To generate the fragments for HC-GGA, the 41S1 genome sequence was first coarsely divided using the following hierarchy: 1) Design fragments no larger than 1,800 bp (including Type IIS recognition sites and spacers), which is a convenient size for cost-effective gene synthesis; 2) minimize potential toxicity from leaky expression driven by bacterial promoters by separating known and suspected bacterial promoters from coding sequences; and 3) where possible, minimize fusion sites within ORFs to ensure most genes were contained within a single fragment. Following these guidelines, a 28-part assembly was chosen, and search windows were defined around the initial division points (*SI Appendix*, Table S2). The circular, BsmBI-domesticated genome was then divided into fragments using the NEBridge SplitSet tool (available at ligasefidelity.neb.com/) to select high fidelity fusion sites (25, 38) with the resulting assembly design having an estimated ligation fidelity of 92% (26) (*SI Appendix*, Fig. S2). To produce the final part sequences, BsmBI recognition sites and a spacer nucleotide were appended to the 5′ and 3′ ends of the SplitSet generated fragments (*SI Appendix*, Table S3).

This approach allowed nearly every fragment to be propagated in *E. coli* cloning strains, despite the known toxicity of some

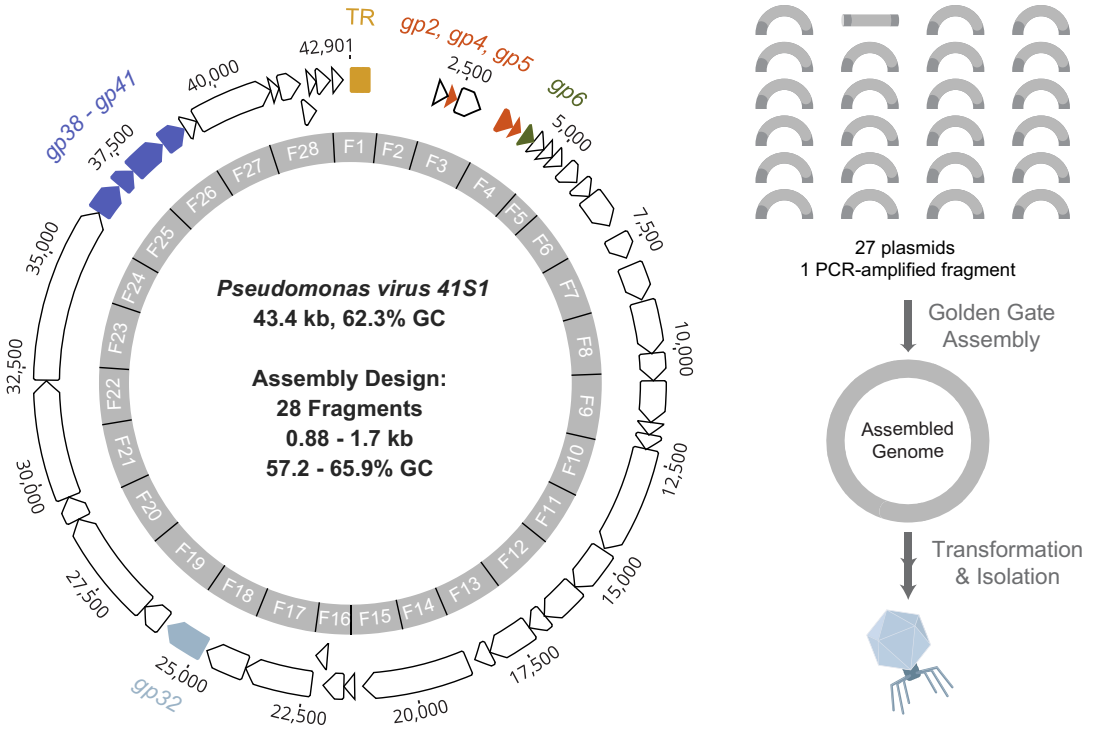

Fig. 1. Design of the 41S1 28-fragment HC-GGA system. The 43.4 kb 41S1 genome was circularized with a single Terminal Repeat (TR, yellow) to yield a 42.9 kb assembly target. The genome was divided into 28 fragments using SplitSet to generate an assembly with 92% estimated fidelity (*SI Appendix*, Fig. S2). Variant assembled were produced by changing the highlighted regions: *gp2*, *gp4,* and *gp5* (orange) had point mutation introduced by SDM, *gp6* (green) was replaced with fluorescent markers, *gp32* (the capsid protein, light blue) had a fluorescent marker added after the gene, *gp38* to *gp41* (blue) were replaced with orthogonal genes from another phiKMV-like phage, and exogenous DNA was inserted between just prior to the Terminal Repeat. The 28 fragments were assembled by GGA and transformed to rescue viral particles. All fragments except F2 were produced as plasmids while F2 was produced by PCR amplification of a synthetic gene fragment.

regions of T7-like phage genomes (22, 3940, 41). In line with prior observations that the most toxic regions are generally those under bacterial promoter control, we found that Fragment 2, encompassing the "ratcheting" region where multiple bacterial promoters in proximity are thought to engage host RNAP upon initial entry, a process which pulls the genome into the cytoplasm (42), could not be maintained in an *E. coli* destination vector. In this case, the promoters may be causing toxicity via excessive RNA generation within the cell. This fragment was obtained as a gene fragment and amplified via PCR to provide enough material for assembly. The remaining 27 fragments were able to be propagated and purified as plasmid DNA, ensuring easy access to large amounts of high purity DNA after the initial establishment of the system. All assembly reactions were carried out using 3 nM of each fragment and using the NEBridge Golden Gate Assembly Kit (BsmBI-v2) following a 15-h assembly protocol (23, 25) and analyzed by TapeStation prior to transformation (*SI Appendix*, Fig. S3).

Synthetic Wild-Type Phage 41S1 Was Reliably Rescued with High Sequence Accuracy. Initial assemblies focused on the Golden Gate-compatible synthetic wild-type 41S1 genome, phAK001, composed of the base assembly fragments (*SI Appendix*, Table S4). Assembled phAK001 was transformed into *P. aeruginosa* cells via electroporation (Fig. 2 *A* and *C*). Transformation efficiency, as measured by plaque formation, was quite variable, with yields of 0 to 1,900 plaques (plaque forming units, PFU) per μg of assembly reaction, with an average of 1,301 PFU/μg of DNA. Variability can likely be attributed to inconsistency in electrocompetent cell quality and the inherent challenges of working with *Pseudomonas* species. Despite this variability, screening of plaques showed a very high success rate in recovery of the phAK001. All plaques analyzed carried the complete genome including all seventeen mutations to remove BsmBI sites.

Approximately 40% of plaques contained errors (primarily single nucleotide polymorphisms and single nucleotide indels), and in ~90% of cases the errors fall within fragment F2—the fragment amplified by PCR from a gene fragment rather than carried in a plasmid (*SI Appendix*, Table S5). We calculated the error rate of F2 as ~1 in 2,500 bp which is roughly consistent with the manufacturer's reported error rate of ~1 in 5,000 bases. This error rate proved tolerable for the single fragment required in this system but would make the isolation of desired sequences challenging as the amount of PCR-amplified synthetic DNA increases. Potential solutions to this issue would be 1) acquiring synthetic DNA from vendors with lower error rates (e.g., Gene Fragments from Twist with an advertised error rate of 1 in 7,500 or ENFINIA Linear DNA from Elegen with an advertised error rate of 1 in 70,000) or 2) after an initial round of rescue and plaque sequencing, isolated gDNA found to be free of errors could be used as the PCR template for future assemblies thereby reducing the error rate to that of high-fidelity PCR. The observed error rate in the portion of the genome assembled from plasmid-derived fragments was less than 1 in 500,000 bases indicating that the cloning of fragments is the optimal strategy when feasible. Even with the limitations of the fragment F2, our results demonstrate the high accuracy and efficiency of this genome synthesis approach, particularly when compared to homology-directed repair methods (11) and is an improvement over recently developed CRISPR-based strategies (13, 43). Our methodology achieves high-fidelity genome reconstruction without the need for selection or counterselection systems.

To address the variability observed in plaque formation following direct transformation into *P. aeruginosa* PAO1, we compared

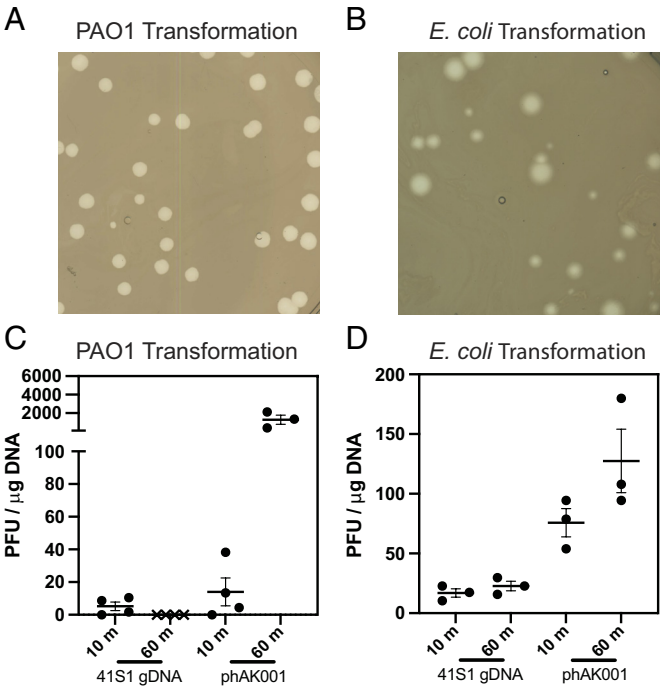

Fig. 2. Transformation and rescue of Golden Gate assembled synthetic wt phage 41S1 in *P. aeruginosa* PAO1 and *E. coli*. Representative plaques after transformation via electroporation of Golden Gate assembled synthetic wt phage 41S1 (phAK001) into *P. aeruginosa* PAO1 (*A*) or into *E. coli* and subsequent coculture with *P. aeruginosa* PAO1 (*B*). Transformation efficiency of $41S1^{648}$ gDNA and phAK001 into *P. aeruginosa* PAO1 (*C*) or into *E. coli* and subsequent coculture with *P. aeruginosa* PAO1 (*D*) after 10 or 60 min of outgrowth before plating. Plots for *C* and *D* represent three or four independent transformations with the mean and SD shown for each.

this approach with an alternative method involving transformation into commercially available electrocompetent *E. coli* cells. We hypothesized that 41S1 phage particles could be produced by *E. coli*, given prior results demonstrating successful rebooting of gammaproteobacteriophages in *E. coli* (17, 44, 45). In this protocol, synthetic 41S1 assemblies were first transformed into *E. coli*, followed by a brief outgrowth period. The resulting culture was then mixed with *P. aeruginosa* PAO1 cells prior to plating. This method yielded robust and consistent plaque formation (Fig. 2 *B* and *D*) with significantly reduced variability compared to direct transformation into *P. aeruginosa*. Moreover, the frequency and types of sequence errors in recovered phage genomes closely mirrored those observed from direct *P. aeruginosa* PAO1. Given its improved reliability, the use of *E. coli* as a surrogate rescue host was adopted for the majority of assemblies described in this study.

To confirm that mutations to remove BsmBI recognition sites from the wildtype genome did not impact phage replication or fitness, we compared the growth curves of *P. aeruginosa* PAO1 cells infected with wild-type (wt) 41S1 phage to those infected with eight plaque lineages of the phAK001 synthetic wt phage (*SI Appendix*, Fig. S4*A*). Growth at 37 °C showed a latent period of 10 to 15 min, followed by lysis between 15 and 20 min, yielding burst sizes of 40 to 60 phage particles. The synthetic phages showed similar behavior to wt phages, indicating that none of the domesticating mutations impacted fitness or replication on *P. aeruginosa* PAO1. Thus, our design approach successfully produced synthetic phage phenotypically indistinguishable from wt phage during *P. aeruginosa* PAO1 infection.

We noted during sequencing of the control samples for this experiment that our wt 41S1 strain (henceforth denoted $41S1^{648}$) had acquired a C206Y mutation in *gp40*, a putative tail fiber gene, relative to the original genome sequence. The mutation in the tail fiber did not noticeably impact the replication cycle, as no differences were noted in wt vs. phAK001 infection of PAO1. Nevertheless, for future experiments we also used a 41S1 strain that lacked the C206Y mutation (denoted as 41S1).

Generation and Characterization of Precise Phage Variants. To test the ability to generate phage strains with precise genomic modifications, we introduced a series of point mutations into fragments F3 and F4 based on sequence alignments of *Phikmvvirus* strain Early genes as a proof of concept for future screening of Early gene libraries (*SI Appendix*, Table S6). These mutations were incorporated into F3 and F4 clones using standard SDM, resulting in a set of alternate parts (*SI Appendix*, Table S3). These modified fragments were then substituted into the base assembly, either individually or in combination, to generate seven alternative assemblies encompassing all possible mutation combinations (phAK002-008, *SI Appendix*, Table S4). Upon transformation and rescue, plaques were obtainable for all variants. Sequencing of eight plaques per variant confirmed consistent recovery of the intended mutations. Out of 56 plaques across all point mutant variants, 100% contained the expected mutations, including the domesticating changes and those introduced in fragments F3 and F4. As observed with phAK001, approximately one-third of plaques carried minor errors, nearly all of which were within fragment F2 (*SI Appendix*, Table S5). All mutant phages tested, whether carrying single or combined mutations, achieved titers comparable to those of $41S1^{648}$ and phAK001 (*SI Appendix*, Fig. S4*B*).

In addition to testing individual assemblies containing specific mutations, we also assembled and transformed a combinatorial mixture of all variant fragments. Transformation with 1 µg of assembled DNA yielded an average of 347 (±51) plaques. The entire plate was scraped, phages were harvested, and genomic DNA was isolated from the pooled population and sequenced. A sample of the assembly reaction was amplified by PCR across F3 and F4 and was sequenced to serve as the pool input. *SI Appendix*, Fig. S5 depicts the distribution of mutation combinations present in both the assembled input and pooled phage population. The genomic distribution of variants reflects both the rescue efficiency and the plaquing characteristics of each mutant. All intended combinatorial mutation variants were recovered, and their relative ratios closely matched that observed in the input sample indicating that the final distribution was dictated by the distribution in the assembly reaction. These results show that multiple 41S1 variants can be rescued from a single combinatorial assembly reaction. While the complexity of the current assembly was small (eight members) our observed transformation efficiency (Fig. 2) would allow for significantly more complex libraries of 41S1 variants, on the order of hundreds to thousands, to be assembled and rescued in parallel with minimal or no scale up.

41S1 Tail Fiber Gene Variants Show Distinct Host Infectivity Across *Pseudomonas* strains. As has been previously demonstrated (46, 47), the engineering of receptor binding proteins (e.g., tail fibers) is a valuable tool in altering phage host range and could assist in the generation of phages suitable for therapeutic use (48). To explore the impact of tail fiber variations in host specificity and growth kinetics with 41S1, we chose to replace a group of genes (*gp38-gp41*) around the putative tail fiber genes, *gp38* and *gp40* (49) (*gp39* and *gp41* are annotated as hypothetical proteins), of 41S1 with the orthogonal genes from another *Pseudomonas Phikmvvirus* vB_PaeP_P1G (GenBank: OQ230793.1, henceforth

P1G) (50). The genomes of 41S1 and P1G are highly similar overall (88% identical) with only a few regions of divergence, primarily in the early genes and genes *gp39* and *gp40*. Alignment of the translated proteins showed that *gp38* and *gp41* have greater than 95% identity, while *gp39* and *gp40* are 53% and 70% identical, respectively, to their P1G homologues (Fig. 3*A*). We designed modified versions of F25 and F26 replacing 41S1 genes *gp38* to *gp41* with the P1G orthologs (*SI Appendix*, Table S3) and generated eight tail fiber gene variants by the substitution of the modified versions of fragments F25 and F26 into the assembly reaction (phAK009-016, *SI Appendix*, Table S4). Assembly reactions were transformed into *E. coli* and cocultured with *P. aeruginosa* strains PAO1 with all variants yielding plaques.

We further assessed the host range of the eight tail fiber-shuffled phages using efficiency of plaquing (EOP) assays (Fig. 3*B*) and growth kinetics (*SI Appendix*, Fig. S6) across a panel of *P. aeruginosa* (*Psa*) strains of clinical, animal, and environmental origins (*SI Appendix*, Table S7). For some of the *P. aeruginosa* strains, tail swaps had minimal impact on EOP [i.e. a log(EOP^{nor}) close to 0]. 41S1 strains phAK009, 010, 012, 013, and 015 failed to plaque on *Psa* strains 3440 and 3447. In contrast, strains phAK009, 010, 012, 013, 015, and 016 showed enhanced plaquing ability on *Psa* strain 3427 when compared to 41S1. These results seem to be driven by the presence of the alternative *gp40* gene. Notably, tail fiber variant phage phAK016, which is the only variant to include the full set of alternative *gp38* to *gp41* genes, retained infectivity on both strains 3440 and 3447 where the other aforementioned tail fiber variants failed to infect these bacterial hosts. Similar patterns are seen with phAK009, 010, 012, 013, 015, and 016 for phage infectivity with low infectivity (high relative AUC^{nor} i.e. greater bacterial growth) on strain 3440 and a higher infectivity (low relative AUC^{nor} i.e. less bacterial growth) relative to that of 41S1 on strain 3414. We also noticed differences in EOP between the two control strains, 41S1 and $41S1^{648}$, on *Psa* strains 3414 and 3427. The presence of the C206Y mutation in *gp40* $41S1^{648}$ appears correlated with alterations in host range; this same mutation appears natively in the *gp40* ortholog from *Pseudomonas* phage P1G.

These results highlight the impact of the genomic context for phage tail fiber variations where even closely related phages may exhibit distinct host interactions due to modular tail fiber gene differences (51). Furthermore, it demonstrates the ability of this approach to functionally replace multiple genes at once, allowing us to ascertain phenotypes of homologous genes in an isogenic background from sequencing data alone (e.g., when a phage isolate is not readily accessible), something that has previously been difficult to do in phage biology.

Synthetic 41S1 Phage Tolerates a Genomic Expansion of 1,500 Base Pairs Without Detectable Phenotypic Changes. To test the size limitation of DNA packaging into phiKMV-like capsids (the 41S1 and phiKMV capsid proteins are 96.7% identical), synthetic phage assemblies were engineered to include increasing lengths of randomly generated, noncoding DNA (0.5, 1.0, 1.5, 2.0, 2.5, 3.0, and 3.5 kb). Insertions were made at the 3′ terminus of the circular genome, following the final terminator and before the terminal repeat in fragment F1. The full 3.5 kb insert sequence was designed in silico to lack promoters and homology to known sequences with GC content similar to the rest of the 41S1 genome and ordered as synthetic, clonal DNA. This plasmid was used as template for SDM to systematically remove sections of the DNA insert to generate the set of plasmids (*SI Appendix*, Table S3). The insert region containing fragments were substituted for F1 in assembly reactions and rescued by transformation into *E. coli* and cocultured with *P. aeruginosa* PAO1 as the host (phAK017-023, *SI Appendix*, Table S4). All assemblies yielded viable phage particles. Eight

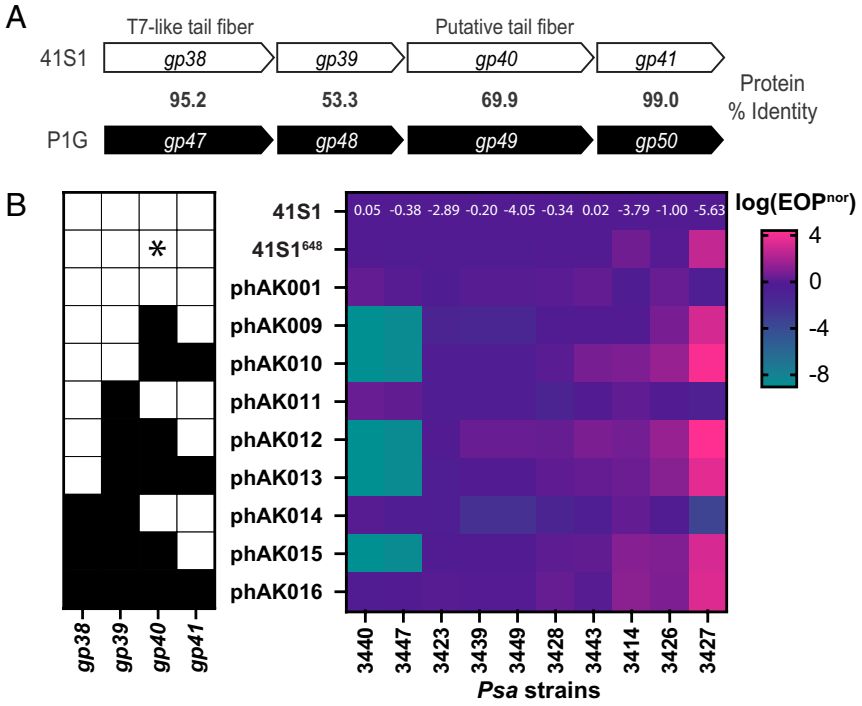

Fig. 3. Altered host range of tail fiber variants. (*A*) Schematic of 41S1 and P1G (abbreviated P1G) genomes near the tail fiber genes with the protein percent identity between orthologs shown. (*B*) Changes in host range of tail fiber variant phages across 10 different *Psa* strains visualized by log efficiency of plaquing (EOP) normalized to the EOP of 41S1 with the 41S1 log(EOP) values on each strain listed in the first row. Values greater than 0 (magenta) indicate a higher log(EOP^{norm}), or increased plaquing ability on a bacterial strain while values less than 0 (blue to teal) indicate a lower log(EOP^{norm}) or decreased plaquing ability. Black squares in the left-hand grid indicate 41S1 genes that have been replaced with their P1G orthologs. The asterisk notes that $41S1^{648}$ contains a C206Y mutation in *gp40* compared to wt 41S1.

plaques from each assembly were isolated, and PCR confirmed the presence of the intended insertions. PCR detection of the insert region from the 41S1 control and lysates derived from assemblies containing between 0.5 to 2.0 kb inserts showed single bands of the expected size (Fig. 4*B*), while those with 2.5 to 3.5 kb inserts showed multiple bands, suggesting deletions in the inserted region which was confirmed by genomic DNA sequencing (*SI Appendix*, Table S5). It remains unclear whether these deletions occurred during phage replication or arose from minor populations in the initial assembly that were selectively amplified due to packaging defects in phages exceeding 2 kb of additional DNA.

To assess long-term stability of the DNA insertion, four lysates retaining the largest insert regions from each assembly were serially passaged for 10 rounds of amplification and analyzed by PCR. Titers remained high across all variants (Fig. 4*C*), indicating minimal fitness defects in the passaged phage lines. As expected, passaged lysates with 2.5 to 3.5 kb inserts showed progressive and multiple deletions of the insert region, with some of the postpassage bands being smaller in size than those observed initially before serial passage (*SI Appendix*, Fig. S7*A*), consistent with ongoing deletions over the course of the experiment. Serially passaged 41S1 phages and assemblies carrying 0.5 to 1.5 kb inserts showed a single band of the expected size, suggesting the insertion of the extra DNA can be stably maintained over time, while the serial passaging of lysates carrying a 2.0 kb insert showed mixed outcomes: some lineages maintained the full insert, while others accumulated deletions. Further analysis of timepoints from the serially passaged 2.0 kb insert lysates (Fig. 4*D* and *SI Appendix*, Fig. S7*B*) showed that deletions occurred at different timepoints during the course of the experiment for each lineage. Deletions were first detected after passages 2, 5, 8, and 6 for lineages A to D, respectively, although full-length genomes were detectable by PCR across the entire experiment and by sequencing in passage 10 lysates. The full-length insert was only overtaken by a truncation in lineage A eight passages after the truncation was first detected. Other assemblies that contained inserts larger than 1.5 kb before serial passage also accumulated deletions during serial passage to bring the increase in genome size below ~1.5 kb with the largest retained inserts after serial passage being 1.6 to 1.7 kb.

Our results suggest that the 41S1 capsid can stably accommodate slightly more than 1.5 kb of additional genetic material—approximately 4% of the size of the genome—without significant fitness defects, the addition of ~2.0 kb of added DNA is marginally stable, and additions larger than 2.0 kb are highly unstable and quickly truncated. The amount of added sequence can be increased by the removal of the nonsense mutation-containing *gp6*, allowing an additional 300 bp of genetic material to be added to 41S1. This permits other functional payloads to be incorporated into the genome, for example, additional antidefense genes, CRISPR arrays targeting host factors, or fluorescent reporter genes (4, 52–54).

We also observed two deletions in areas outside of the insert region after serial passage. First, in the phAK021 lineage C sample a portion of *gp48* was lost along with part of the insert region. Second, in the phAK021 lineage D sample the entirety of *gp48* and a portion of *gp47* were lost along with part of the insert region. This allows us to infer that *gp47* and *gp48* are not essential to 41S1. Point mutations in *gp40* were also observed after serial passage which are discussed in *SI Appendix*, *Discussion*.

Construction of Fluorescent Reporter Phages Using Synthetic 41S1. Building on our previous experiments demonstrating successful tail fiber gene swapping and the approximate size limit of the capsid, we next evaluated the ability to incorporate and express functional coding sequences by inserting fluorescent protein genes into the 41S1 genome. Two versions of fluorescent

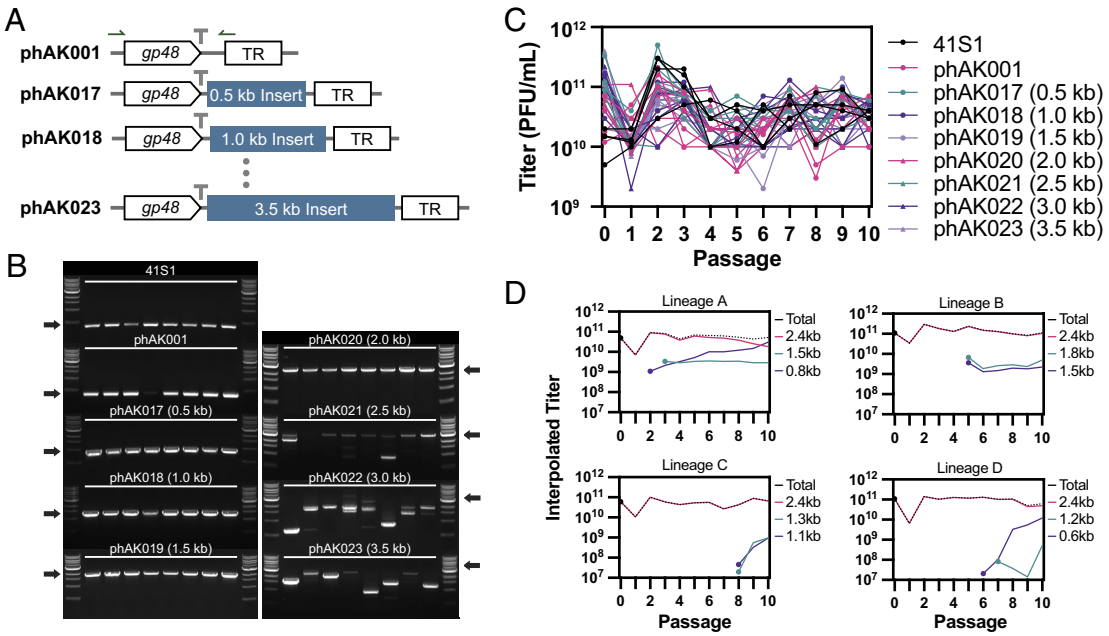

Fig. 4. Incorporation and stability of excess DNA in the 41S1 genome. (*A*) Schematic of the variably sized insert regions in fragment F1. Native genome features are shown in black outline with the excess DNA inserted between *gp48* and the 3′ terminal repeat (TR) and the *gp48* terminator shown in gray. The inserted DNA is shown in blue. The locations of the primers used for panels *C* and *D* are shown in green. (*B*) Agarose gels of PCR amplicons of the DNA insert region for eight independent lysates of 41S1, phAK001, and assemblies with 0.5 to 3.5 kb of inserted DNA (phAK017 to 023). Arrows indicate the expected amplicon size for each genome. All gels used NEB 1 kb DNA ladder (N3232) for size assessment. (*C*) Phage titers of passaged phages. (*D*) Interpolated phage titers of the four independent phAK020 (2.0 kb insert) assembly lysates over 10 passages. Gels of PCR amplicons for each passage (*SI Appendix*, Fig. S7*B*) were analyzed by densitometry relative to the band at passage 0. The resulting ratios of bands were applied to the measured phage titer at passage 0 from Panel *C*. The 2.4 kb population represents the full 2.0 kb insertion with smaller sizes representing truncated populations labeled by PCR band size. Circles mark the first passage in which a population was detected.

protein expressing 41S1 were designed. The first fused a superfolder GFP (sfGFP) to the C-terminus of the major capsid protein, *gp32* (phAK024). The second incorporated two fluorescent proteins into the genome, an mScarlet-I3 replacing *gp6* and a nonfused sfGFP downstream of *gp32* (phAK025).

The closely related *E. coli* phage T7 readily tolerates fusions on the minor capsid protein (53), which is produced by a frame-shift during capsid translation ~10% of the time (55). However, phiKMV-like phages only produce a single capsid isoform and consequently lack a minor capsid protein to use as a fusion site. Thus, fusions made to the capsid will be present on every molecule of the capsid protein. Initial attempts to directly fuse sfGFP to the C terminus of *gp32* within fragment F19 failed to produce plaques, suggesting that the fusion disrupted capsid assembly or function. To overcome this, we inserted a copy of the *gp32-sfGFP* fusion in place of the nonsense mutation containing Early gene *gp6* in fragment F4 to serve as a "minor capsid protein" and restored the unmodified *gp32* in F19 to generate phAK024. For a second reporter strategy, an mScarlet-I3 gene was inserted in place of *gp6*, and an sfGFP gene was added downstream of *gp32*, both under control of T7 ribosome binding sites to generate phAK025. Both modified assemblies were successfully rescued upon transformation and sequencing confirmed the intended genotypes (*SI Appendix*, Table S5).

To confirm functional expression of the fluorescent proteins during the phage growth cycles of phAK024 and phAK025, fluorescence and OD_{600} were monitored from 2 to 10 h post infection. In phAK024-infected cultures, sfGFP fluorescence showed a strong peak during active infection and declined following host lysis (Fig. 5*A*). Similarly, in phAK025, both sfGFP and mScarlet-I3

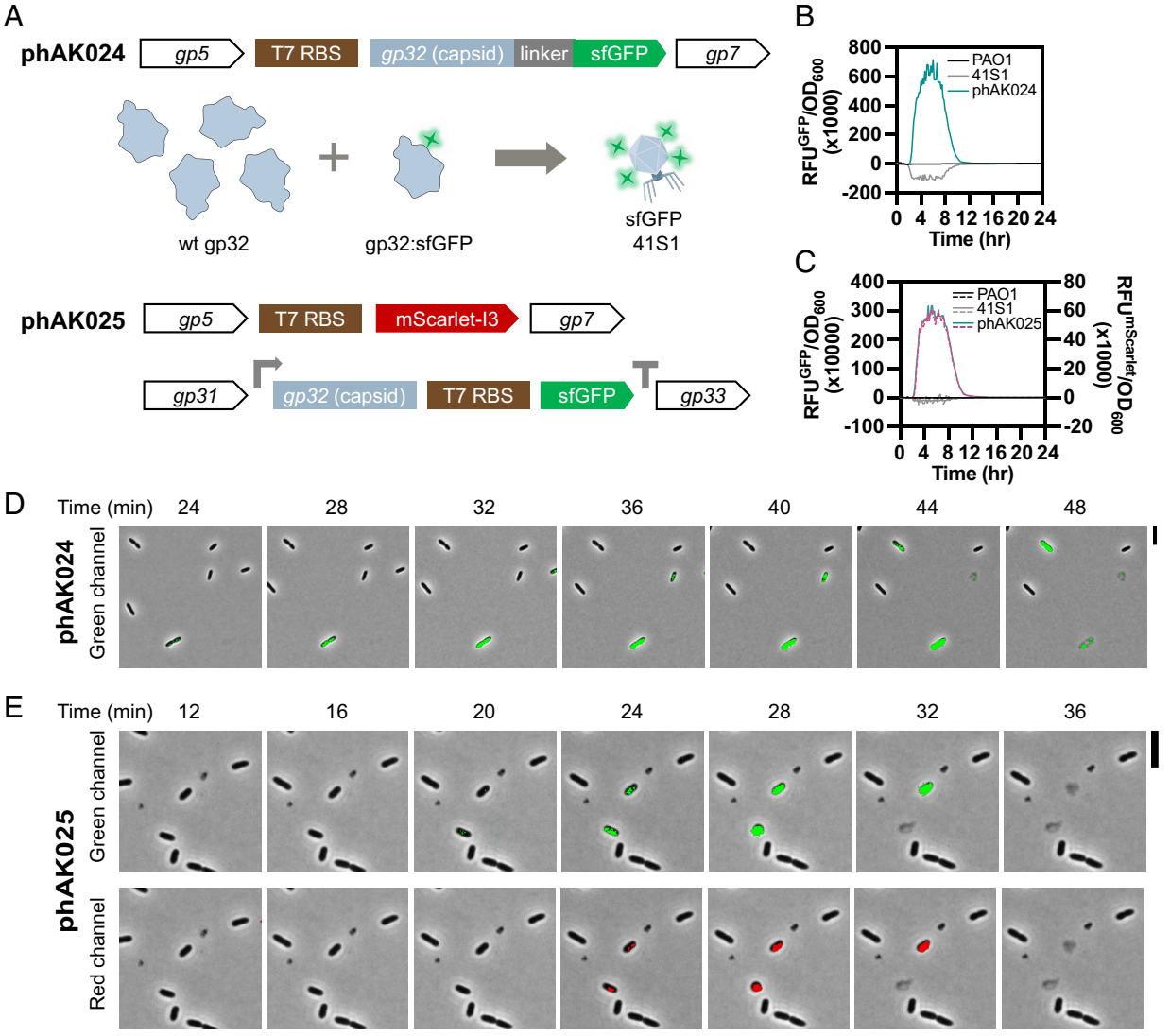

Fig. 5. Infection dynamics of fluorescent 41S1. (*A*) Modifications to the 41S1 genome in phAK024 and phAK025. In phAK024, *gp6* is replaced with a *gp32:sfGFP* gene under a T7 RBS. The results in the production of a capsid protein with a C-terminal sfGFP fusion in addition to wt capsid. These combine to produce sfGFP-labeled viral particles. In phAK025, *gp6* is replaced with an mScarlet-I3 gene under a T7 RBS and an sfGFP gene is inserted after *gp32* resulting in red and green fluorescent markers in infected cells. For both, native genes are shown in black outline; the *gp32* promoter and terminator are shown in gray. (*B*) Growth of phage and bacteria (PAO1 alone, black; 41S1, gray; and phAK024, teal) visualized as OD_{600} normalized expression of GFP tagged capsid. (*C*) Growth of phage and bacteria visualized as OD_{600} normalized expression of GFP on the left *y*-axis (PAO1 alone, black; 41S1, gray; and phAK025, teal) and OD_{600} normalized expression of mScarlet on the right y-axis (PAO1 alone, dashed black; 41S1, dashed gray; and phAK025, dashed magenta). (*D*) Images show bacteria infected with phAK024 at 4-min intervals, starting from t = 24 min postinfection. (*E*) Images show bacteria infected with phAK025 at 4-min intervals, starting from t = 12 min postinfection. Filtered fluorescent signals (green or red) are overlaid on phase-contrast images. Infected cells exhibit increasing fluorescence intensity over time, followed by cell lysis visible in the phase-contrast channel. (Scale bar, 5 μm.) Complete time-lapse sequences showing a few additional cells from our dataset, with combined phase-contrast and fluorescent channels, are available in Movies S1 and S2.

signals were detectable and followed similar temporal dynamics (Fig. 5*B*), despite being under control of promoters associated with different stages of the phage lifecycle.

With the successful production of fluorescent proteins by our reporter phages, we further tested if these strains allow for microscopic visualization of phage infection dynamics without the use of exogenous dyes. Microscopic visualization of infection dynamics was performed using *P. aeruginosa* PAO1 cells infected with either phAK024 or phAK025 (Movies S1 and S2). Time-lapse imaging of phAK024 infecting *P. aeruginosa* PAO1 (Fig. 5*C*) shows cytosolic GFP expression beginning ~20 min postinfection, followed by lysis and the appearance of localized GFP puncta which remain localized to the position of the infected cells, likely representing gp32-sfGFP fusion proteins incorporated into phage capsids. These puncta remained spatially confined, suggesting limited diffusion postlysis. Similarly, phAK025 infection of *P. aeruginosa* PAO1 cells (Fig. 5*D*) showed increasing sfGFP and mScarlet-I3 signals in two individual infected cells, followed by lysis and dispersal of the fluorescent signal. Notably, both signals were detected in synchrony, despite being driven by promoters associated with different stages of the phage infection cycle which is discussed further in *SI Appendix*, *Discussion*. Nonetheless, our results show that synthetic phiKMV-like phages can stably incorporate and express functional fluorescent proteins, enabling real-time visualization of infection dynamics without exogenous dyes.

Conclusions

Here we report the successful production and engineering of infectious 41S1 phage particles derived entirely from synthetic DNA, demonstrating that our HC-GGA modular design principles are applicable to phages beyond the previously established *E. coli* T7 phage model system (23). The genome was divided into small DNA fragments to allow for cost-effective synthesis, most of which were compatible with pUC origin *E. coli* vectors permitting the straightforward preparation of large amounts of high purity DNA for little additional cost. The small fragment size and compatibility with *E. coli* means parts can be easily modified via standard molecular biology methods or inexpensively replaced with new synthetic parts, enabling simple gene mutagenesis or replacement. We demonstrate the simple and reliable incorporation of precise point mutations, large insertions, gene swaps, and the inclusion of additional functional genes into the 41S1 genome that are expressed during the infection cycle. Our strategy also allows for fast turnaround of engineered genomes and for many engineered genomes able to be assembled in parallel. In theory, these design principles can be extended to any phage genome up to ~50 kb that can be rescued from a circular genomic form, see *SI Appendix*, Discussion for more detail. Moreover, the ability to rescue a phage genome assembly directly into *P. aeruginosa,* a host with low transformation efficiency, suggests that this strategy is broadly applicable to diverse bacterial species. The protocol could, in principle, be applied to generate a large mutant library without the need for highly engineered selection tools or marker genes which could interfere with phage viability. Importantly, the capability to generate genomes from fully synthetic DNA demonstrates that only the genome sequence and knowledge of the host are required, eliminating the need for a phage isolate and enabling the construction of uncultivated or metagenomically identified phage genomes. Thus, one-pot phage genome synthesis has the potential to significantly expand the number of phages available for research of phage biology as well as phage-based therapeutic or other biotechnology development.

Methods and Materials

Bacterial Strains and Growth Conditions. A complete list of strains used in this study can be found in *SI Appendix*, Table S7. Both *E. coli* and *P. aeruginosa*, were routinely grown in Luria–Bertani Miller (LB, MP Biomedicals) broth with 200 rpm shaking and LB agar at 37 °C. Where necessary, LB medium (MP Biomedicals Cat. No. 3002042) was supplemented with 10 mM $MgSO_4$ (LB-M).

In Silico 41S1 Genome Assembly Design. A 43,365 bp phiKMV-like phage 41S1 (genus *Phikmvvirus*) isolated from sewage sample from New Haven, CT (GenBank: PX380000) (56, 57) was used as the basis for the assembly design. The linear genomic DNA sequence was first circularized including a single copy of the 464-nucleotide terminal repeat region resulting in a 42,901 bp sequence. Native BsmBI sites in intragenic regions were removed by silent mutations following a codon usage table for *P. aeruginosa* PAO1 (37). BsmBI sites in intergenic regions were removed by comparison to related *Phikmvvirus* sequences and modified to conserved sequences that lack BsmBI sites (*SI Appendix*, Table S1 and Fig. S1). Using the previously reported methodology for selecting high fidelity sets of breakpoints (25, 26) the genome was divided into 28 fragments using SplitSet (*SI Appendix*, Table S2). Fragment sequences output by SplitSet had BsmBI recognition sites and spacers appended to the 5′ and 3′ ends to generate the desired overhangs (*SI Appendix*, Table S3).

Derivative assemblies were designed modifying these core fragments (*SI Appendix*, Table S3). Plasmids F25.2, F25.3, F26.2, and F26.3 were created by replacing the indicated genes in the core fragments with the homologous genes from *Pseudomonas* phage vB_PaeP_P1G (GenBank: OQ230793.1) (58). Plasmid F1.2 was created by inserting 3.5 kb of random DNA sequence between the terminator following *gp48* and the terminal repeat region. The DNA sequence was generated using DNA Chisel (59) to be free of Type IIS recognition sites, homopolymer repeats, hairpins, and to have GC content of ~62%, matching 41S1. Strong promoter regions were detected using SAPPHIRE.CNN (56) and removed by base changes within the predicted promoters. Last, validated primer sites [primers P1 to P7 from Lund et al. (58)] were added every 500bp to allow for the deletion of defined portions of the insert region by SDM. Plasmid F4.5 was created by replacing part of the intergenic region between *gp5* and *gp6* and all of *gp6* with and a *gp32* (capsid gene)-*sfGFP* fusion gene under a T7 Ribosome Binding Site (RBS). Plasmid F4.6 was created in the same manner except an mScarlet-I3 gene was inserted in place of the *gp32-sfGFP* fusion. Plasmid F19.2 was created by inserting a T7 RBS site and sfGFP gene after *gp32* and prior to the capsid terminator.

Synthetic DNA Fragments. Most fragment sequences were ordered as synthetic DNA inserted into the EcoRV site of pUC57-mini derivative holding vectors (see *SI Appendix* Table S8 for vector sequences) from GenScript. For portions of the genome that were not suspected to contain DNA under bacterial promoters (i.e., the late genes), a Type IIS site free derivate of the pUC57-mini vector (GenScript) was chosen. For the early and mid-genes, a new pUC57-mini derived vector was created that contains strong terminators upstream (rrnB T1) and downstream (a reversed rrnC) of a multiple cloning site dubbed pTMT (Terminator-MCS-Terminator). Twenty-seven of twenty-eight fragments were able to be produced in this manner. Plasmids obtained from GenScript were ordered at maxiprep-scale as lyophilized DNA and were resuspended in 100 μL of nuclease-free water. Plasmid F1.2, containing the 3.5 kb insert region, was obtained from Ansa Biotechnologies in plasmid pANSA3. Plasmid F1.2 and plasmids generated by SDM were transformed into NEB10-beta cells (NEB, C3019) and plasmid DNA purified using a Plasmid *Plus* Midi Kit (Qiagen, 12943) per the manufacturer's protocol. Purified plasmid sequences were verified by whole plasmid sequencing prior to use in assembly reactions.

The remaining fragment, F2, that was unable to be cloned into pTMT had M13/pUC primer sites appended outside of the BsmBI site and was obtained as a gBlock (IDT). F2 was amplified by PCR before use in assemblies using Q5 Hot Start High-Fidelity 2X Master Mix (NEB, M0494) using the M13/pUC primer sequences found in *SI Appendix*, Table S9. Amplification was performed using 0.5 μM final primer concentrations and 0.1 ng template DNA per 50 μL of reaction. Amplicon DNA was purified using the Monarch DNA Gel Extraction Kit (NEB, T1020) and checked for purity using a Bioanalyzer 2100 and DNA 12000 kit

(Agilent, 5067-1508), see *SI Appendix*, Fig. S8. DNA concentration for all DNA fragments was determined by Qubit quantification using Qubit 1X Broad Range Assay Kit (ThermoFisher, Q33265).

Site-Directed Mutagenesis. Plasmids F1.3-1.8, F3.2, F4.2, and F4.3 were generated using the Q5 SDM Kit (NEB, E0552) and plasmid F4.4 was generated using the QuikChange Lightning Multi SDM Kit (Agilent, 210516) following the manufacturer's protocol. See *SI Appendix*, Table S9 for primer sequences. Plasmid sequences were verified by whole plasmid sequencing.

Phage Genome Golden Gate Assembly and Analysis. For each assembly (*SI Appendix*, Table S4), quantified input fragments were combined into fragment master mixes with equimolar amounts of each fragment. Assembly reactions were set up using the NEBridge Golden Gate Assembly Kit (BsmBI-v2) (NEB, E1602) as follows: 2 μL 10X T4 DNA Ligase Buffer, 2 μL BsmBI-v2 NEBridge Golden Gate Enzyme Mix (a mixture of BsmBI-v2 and T4 DNA Ligase), 3 nM of the fragment master mix (i.e., the final concentration of all fragments in assembly reaction is 3 nM), and nuclease-free water to 20 μL. Assemblies were carried out using a 15-h cycling protocol [(42 °C, 5 min → 16 °C, 5 min) × 90 cycles → 60 °C, 5 min] to achieve maximum assembly yield. One μL samples of assembly reactions were analyzed by TapeStation using a Genomic DNA ScreenTape (Agilent, 5067-5365) to confirm the presence of high MW DNA and the absence of lower MW bands aside from the roughly 2 kb band representing the holding vector backbones (*SI Appendix*, Fig. S3). Concentrations of each assembly were determined with Qubit 1X Broad Range Assay Kit. These assembly reactions were used in the subsequent transformations without further manipulation.

For the combinatorial assembly, the fragment master mix contained a 1:1 mixture of plasmids F3 and F3.2 (i.e., each fragment at 1.5 nM in the assembly reaction) and a 1:1:1:1 mixture of plasmids F4, F4.2, F4.3, and F4.4 (i.e., each fragment at 0.75 nM in the assembly reaction), see *SI Appendix*, Table S4. 1 μL of the combinatorial assembly reaction was used as PCR template with primers spanning from fragments 2 to 5 (pr41S1-9 and pr41S1-10, *SI Appendix*, Table S9) to quantify the pretransformation ratios of the different potential assembly outcomes.

Preparation of Electrocompetent *P. aeruginosa*. A single colony of *P. aeruginosa* PAO1 was inoculated into 18 mL of LB and grown overnight at 42 °C with aeration at 200 rpm. Cells were centrifuged at 4,000×*g* for 15 min at RT. The supernatant was decanted and aspirated without disturbing the cell pellet. The cell pellet was washed three times with 1 mL of filter-sterilized, prechilled 300 mM sucrose. After the final wash, cells were centrifuged and resuspended in 0.7 mL of 300 mM sucrose. Competent cells were divided into 100 μL aliquots and used immediately for electroporation.

Rescue of *P. aeruginosa* Phage 41S1 Assemblies. Approximately 1 μg of DNA from an assembly reaction was added to either 100 μL of freshly prepared *P. aeruginosa* PAO1 electrocompetent cells or 50 μL of NEB 10-beta (*E. coli*) electrocompetent cells (C3020, diluted 1:2 in cold 20% glycerol). The mixture was vortexed briefly and transferred to electroporation cuvettes (0.2 cm gap for PAO1; 0.1 cm gap for *E. coli*), followed by a 10-min incubation on ice. Electroporation was performed using a BioRad MicroPulser at 3.0 kV for PAO1 and 1.8 kV for *E. coli*. Immediately after electroporation, 1 mL of LB-M was added to the electroporation cuvette, and the contents were transferred to sterile culture tubes. Transformants were recovered at 37 °C with shaking at 200 rpm for 1 h (*P. aeruginosa*) or 10 min (*E. coli*).

Following recovery, 200 μL of an overnight culture of PAO1 was added to the 1 mL of recovered transformants and combined with 8 mL of molten top layer (LB-M with 0.7% agar) equilibrated to 50 °C. Mixture was vortexed and immediately spread on a plate (LB-M with 1.5% agar). After 10 min of solidifying at RT, plates were inverted and incubated at 37 °C overnight. Individual plaques were picked into 100 μL of sterile SM buffer (50 mM Tris pH 7.5, 8 mM $MgSO_4$, 100 mM NaCl) and incubated for 1 h at 37 °C with shaking at 200 rpm. To increase titer, resuspended plaques in SM buffer were then added to 3 mL of an early log-phase *P. aeruginosa* PAO1 culture growing in LB-M at 37 °C with constant aeration at 200 rpm. When clearance of the culture was observed (~2 h), cell debris was pelleted at 4,000×*g* for 10 min at RT. The lysate was further clarified by filtration through 0.2 μm pore-size membranes. A 0.5 mL aliquot of the filtered supernatant was used for genomic DNA (gDNA) extraction.

gDNA Extraction and Sequencing. For the source 41S1 genome sequence, a 0.5 mL aliquot of filter-sterilized lysate was treated with 10 μg/mL RNase (NEB, T3018) and DNaseI (ThermoFisher, EN0521) and incubated for 1 h at 37 °C. gDNA was then extracted using a modified protocol based on the Promega Wizard DNA Clean-Up Kit. Briefly, the nuclease-treated lysate was mixed with 1 mL of DNA purification resin by gentle inversion and loaded into a 3 mL syringe fitted with a Wizard Minicolumn. The column was washed with 2 mL of 80% isopropanol, and gDNA was eluted with 50 μL of nuclease-free water preheated to 80 °C by centrifugation at 13,000×*g* for 1 min at RT. DNA concentration was quantified using a Qubit fluorometer, and 500 ng of purified gDNA was submitted for Illumina MiSeq sequencing at SeqCenter (Pittsburgh, PA).

For all other samples, a 0.5 mL aliquot of filter-sterilized lysate was treated with 20 μL of Proteinase K (NEB, P8107) at 56 °C with 300 rpm mixing for 45 min. Next, 260 μL of SPRIselect beads (Beckman Coulter, B23317) were added and the sample was mixed by inversion for 5 min at room temperature. Beads were separated using a magnetic stand, the supernatant was discarded, and the beads were washed 2× using 500 μL of 80% ethanol. Samples were spun, placed on a magnetic stand again, and excess ethanol removed. DNA was eluted with 15 μL of nuclease free water at 37 °C for 5 min before magnetic separation and recovery of the supernatant. DNA concentration was quantified using a Qubit fluorometer and 400 ng of purified gDNA was used as input for the Oxford Nanopore Technologies (ONT) Native Barcoding Kit (SQK-NBD114.24 or SQK-NBD114.96) and sequenced on R10.4.1 flow cells using a GridION sequencer. Sequenced genomes were compared to the assembly target sequence and mutations are noted in *SI Appendix*, Table S5.

For the combinatorial assembly, phage particles were harvested by scraping the top agar from three independent plates, briefly vortexing the pooled top agars, centrifugation for 15 min at 3,000×*g*, and filter sterilization of the supernatant. DNA was prepared for ONT sequencing as above. The combinatorial assembly pretransformation PCR sample (see above) was sequenced by ONT following the same protocol. Reads from pre- and posttransformation samples were then classified as phAK001-008 to determine the ratios of each strain in the samples.

Spot Titer and Efficiency of Plaquing (EOP) Assays. Phage titers were enumerated via spot titer assays. Briefly, 200 μL of an overnight culture of bacteria was added to 8 mL of molten top layer (LB-M with 0.7% agar) equilibrated to 50 °C. Mixture was vortexed and immediately spread on a plate (LB-M with 1.5% agar). After 10 min of solidifying at room temperature (RT), phage was 10-fold serially diluted in phosphate buffered saline (PBS) and 2 to 10 μL of each dilution was spotted on top of the plate. After drying, plates were incubated at 37 °C overnight.

To evaluate the efficiency with which the phages could infect *P. aeruginosa* strains, EOP assays were used. Phages were spot titered on experimental strains of bacteria and PAO1 as described above. EOP was calculated by dividing the titer of phage on the experimental strain by the titer of the same phage on PAO1. Relative EOP was then calculated by dividing the EOP of the phage by the EOP of 41S1 on the same strain.

Phage Growth Curve Assay. Approximately 10^4 PFU of phage were added to a 5 mL culture of *P. aeruginosa* PAO1 at 600 nm optical density (OD_{600}) of ~0.1. Immediately after addition, a 50 μL aliquot of the culture was taken, diluted 1:4 in ice-cold PBS and filter-sterilized to remove bacterial cells. The culture was then incubated at 37 °C, with constant shaking at 200 rpm. Subsequent 50 μL aliquots were collected every 5 min, diluted, and filter-sterilized as described above. Filtered samples were used to enumerate free phage particles by spot titer assays. Experiments were performed in duplicate.

Growth Kinetics Assay. Growth curves in 384 well plates were initiated by adding ~10^9 PFU/mL to 50 μL of a bacterial culture diluted to OD_{600} 0.05. Plates were grown in a BioTek Synergy plate reader for 24 h with constant orbital shaking at 37 °C and OD_{600} was measured every 10 min. The area under the curve (AUC) was calculated by integrating the bacterial growth curve over a 24-h period. To assess the impact of phage lysis, a relative AUC was determined by dividing the AUC of each phage–strain combination by the corresponding AUC of the no-phage control for the same given strain. To enable comparison across experiments, the

resulting relative AUC values were normalized to the relative AUC of the reference phage 41S1 for each strain tested.

Monitoring Stability of Insert Region by PCR. To monitor the stability of the insert region primer sites were chosen upstream and downstream of the insert region (see pr41S1-18 and pr41S1-19, *SI Appendix*, Table S9) that produce a 403 bp amplicon on wild type genomes. The size of the insert region can be determined by subtracting 403bp from the observed amplicon size. Lysate samples were diluted 1:10 with nuclease free water, heated at 95 °C for 10 min, and 1 μL was used as PCR template. Reactions were carried out using 2× GoTaq Green Master Mix (Promega, M7122) and visualized on 1% agarose gels.

Microscopy. Bacterial cultures of *P. aeruginosa* PAO1 were grown overnight in LB at 37 °C. The culture was diluted 1:100 in fresh LB and incubated for 3 h at 37 °C with 200 rpm shaking until reaching exponential phase of growth. Then, 50 μL of bacterial culture (~10^7 CFU) was mixed with 5 μL of phage stock (~10^8 PFU) in a microcentrifuge tube. A 10 μL aliquot of this mixture was spotted on an LB + 1.5% agarose pad prepared in a cavity slide (Thomas Scientific, 1201A73). A #1.5 coverslip (Fisher Scientific, 12-541B) was placed over the sample, and the slide was incubated at 37 °C for 8 to 10 min to promote edge evaporation and eliminate fluid flow within the agarose pad. The coverslip was then sealed on all sides with VALAP (a 1:1:1 mixture of Vaseline, lanolin, and paraffin wax) to prevent further evaporation. Imaging was conducted at 37 °C using a Nikon Ti-E inverted microscope equipped with a temperature-controlled chamber and a 100× oil immersion objective (NA 1.40). Images were acquired every 15 s (4 frames/min) using phase-contrast, GFP, and RFP channels.

Data, Materials, and Software Availability. Genome sequence data for 41S1 have been deposited in GenBank (PX380000) (57). All other data are included in the manuscript and/or supporting information. Complete sequence files for plasmids and synthetic 41S1 genomes have been deposited on Dryad (60).

Author affiliations: [a]Applied Molecular Biology Division, New England Biolabs Research Department, Ipswich, MA 01938; [b]Department of Ecology and Evolutionary Biology, Yale University, New Haven, CT 06511; [c]Center for Phage Biology & Therapy, Yale University, New Haven, CT 06511; [d]Felix Biotechnology, San Francisco, CA 94080; and [e]Yale School of Medicine, Microbiology Graduate Program, New Haven, CT 06510

Author contributions: A.P.S., K.E.K., H.S., M.H., R.M., and G.J.S.L. designed research; A.P.S., K.E.K., H.S., J.A., M.D., M.H., B.N., C.A.S.-V., and S.K.T. performed research; B.K.C. and P.E.T. contributed new reagents/analytic tools; A.P.S., K.E.K., J.A., V.P., C.A.S.-V., and S.K.T.analyzed data; and A.P.S., K.E.K., P.E.T., and G.J.S.L. wrote the paper.

Reviewers: J.E.B., Michigan State University; and T.K.L., Massachusetts Institute of Technology.

Competing interest statement: A.P.S., B.N., V.P., C.A.S.-V., S.K.T., and G.J.S.L. are employees of New England Biolabs, a manufacturer and vendor of molecular biology reagents, including DNA ligases, Type IIS restriction enzymes, and DNA assembly kits. This affiliation does not affect the authors' impartiality, adherence to journal standards and policies, or availability of data. H.S. and M.H. are former employees, and R.M. and P.E.T. are former cofounders, of Felix Biotechnology, a company that is no longer operating but sought to commercially develop phages for human therapy.

1. S. T. Abedon, P. García, P. Mullany, R. Aminov, Editorial: Phage therapy: Past, present and future. *Front. Microbiol.* **8**, 981 (2017).
2. O. Alessa *et al.*, Synthetic and functional engineering of bacteriophages: Approaches for tailored bactericidal, diagnostic, and delivery platforms. *Molecules* **30**, 3132 (2025).
3. M. A. Elois, R. D. Silva, G. V. T. Pilati, D. Rodríguez-Lázaro, G. Fongaro, Bacteriophages as biotechnological tools. *Viruses* **15**, 349 (2023).
4. H. Peng, I. A. Chen, U. Qimron, Engineering phages to fight multidrug-resistant bacteria. *Chem. Rev.* **125**, 933–971 (2025).
5. S. A. Strathdee, G. F. Hatfull, V. K. Mutalik, R. T. Schooley, Phage therapy: From biological mechanisms to future directions. *Cell* **186**, 17–31 (2023).
6. A. R. Mushegian, Are there 10^{31} virus particles on Earth, or more, or fewer? *J. Bacteriol.* **202**, e00052-20 (2020).
7. A. P. Camargo *et al.*, IMG/VR v4: An expanded database of uncultivated virus genomes within a framework of extensive functional, taxonomic, and ecological metadata. *Nucleic Acids Res.* **51**, D733–D743 (2022).
8. B. K. Chan, S. T. Abedon, C. Loc-Carrillo, Phage cocktails and the future of phage therapy. *Fut. Microbiol.* **8**, 769–783 (2013).
9. Y. Chen *et al.*, Genetic engineering of bacteriophages against infectious diseases. *Front. Microbiol.* **10**, 954 (2019).
10. M. Mahler, A. R. Costa, S. P. B. van Beljouw, P. C. Fineran, S. J. J. Brouns, Approaches for bacteriophage genome engineering. *Trends Biotechnol.* **41**, 669–685 (2023).
11. L. J. Marinelli *et al.*, BRED: A simple and powerful tool for constructing mutant and recombinant bacteriophage genomes. *PLoS ONE* **3**, e3957 (2008).
12. B. Martel, S. Moineau, CRISPR-Cas: An efficient tool for genome engineering of virulent bacteriophages. *Nucleic Acids Res.* **42**, 9504–9513 (2014).
13. K. S. Wetzel *et al.*, CRISPY-BRED and CRISPY-BRIP: Efficient bacteriophage engineering. *Sci. Rep.* **11**, 6796 (2021).
14. C. S. Kristensen, A. Petersen, M. Kilstrup, E. Helm, A. Takos, Cell-free synthesis of infective phages from in vitro assembled phage genomes for efficient phage engineering and production of large phage libraries. *Synth. Biol. (Oxf.)* **9**, ysae012 (2024).
15. A. Levrier *et al.*, PHEIGES: All-cell-free phage synthesis and selection from engineered genomes. *Nat. Commun.* **15**, 2223 (2024).
16. C. C. Koster, E. D. Postma, E. Knibbe, C. Cleij, P. Daran-Lapujade, Synthetic genomics from a yeast perspective. *Front. Bioeng. Biotechnol.* **10**, 869486 (2022).
17. H. Ando, S. Lemire, P. Pires Diana, K. Lu Timothy, Engineering modular viral scaffolds for targeted bacterial population editing. *Cell Syst.* **1**, 187–196 (2015).
18. X. Forns, J. Bukh, R. H. Purcell, S. U. Emerson, How *Escherichia coli* can bias the results of molecular cloning: Preferential selection of defective genomes of hepatitis C virus during the cloning procedure. *Proc. Natl. Acad. Sci. U.S.A.* **94**, 1394–1399 (1997).
19. C. M. Thomas, "Genetic manipulation of bacteria" in *Biotechnology Vol. III*, H. W. Doelle, S. Rokem, M. Berovic, Eds. (EOLSS Publishers, Oxford, UK, 2009).
20. E. M. Pulkkinen, T. C. Hinkley, S. R. Nugen, Utilizing *in vitro* DNA assembly to engineer a synthetic T7 Nanoluc reporter phage for *Escherichia coli* detection. *Integr. Biol.* **11**, 63–68 (2019).
21. C. M. Mageeney *et al.*, Computational basis for on-demand production of diversified therapeutic phage cocktails. *mSystems* **5**, e00659-20 (2020).
22. J. Liang, H. Zhang, Y. L. Tan, H. Zhao, E. L. Ang, Directed evolution of replication-competent double-stranded DNA bacteriophage toward new host specificity. *ACS Synth. Biol.* **11**, 634–643 (2022).
23. J. M. Pryor, V. Potapov, K. Bilotti, N. Pokhrel, G. J. S. Lohman, Rapid 40 kb genome construction from 52 parts through data-optimized assembly design. *ACS Synth. Biol.* **11**, 2036–2042 (2022).
24. H. Zhang *et al.*, Programming virulent bacteriophages by developing a multiplex genome engineering method. *mBio* **16**, e03582-24 (2025).
25. A. P. Sikkema, S. K. Tabatabaei, Y.-J. Lee, S. Lund, G. J. S. Lohman, High-complexity one-pot Golden Gate assembly. *Curr. Protoc.* **3**, e882 (2023).
26. J. M. Pryor *et al.*, Enabling one-pot Golden Gate assemblies of unprecedented complexity using data-optimized assembly design. *PLoS ONE* **15**, e0238592 (2020).
27. C. C. Ko *et al.*, Genome synthesis, assembly, and rebooting of therapeutically useful high G+C% mycobacteriophages. *Proc. Natl. Acad. Sci. U.S.A.* **122**, e2523871122 (2025).
28. R. Lavigne *et al.*, Pseudomonas phage phiKMV. National Center for Biotechnology Information. https://www.ncbi.nlm.nih.gov/nuccore/AJ505558.1. Accessed 20 December 2025.
29. R. Lavigne *et al.*, The genome of bacteriophage φKMV, a T7-like virus infecting *Pseudomonas aeruginosa*. *Virology* **312**, 49–59 (2003).
30. B. R. Lenneman, J. Fernbach, M. J. Loessner, T. K. Lu, S. Kilcher, Enhancing phage therapy through synthetic biology and genome engineering. *Curr. Opin. Biotechnol.* **68**, 151–159 (2021).
31. P.-J. Ceyssens, R. Lavigne, Bacteriophages of *Pseudomonas*. *Fut. Microbiol.* **5**, 1041–1055 (2010).
32. V. N. Krylov, "Bacteriophages of *Pseudomonas aeruginosa*: Long-Term prospects for use in phage therapy" in *Advances in Virus Research*, K. Maramorosch, F. A. Murphy, Eds. (Academic Press, 2014), pp. 227–278.
33. S. Qin *et al.*, *Pseudomonas aeruginosa*: Pathogenesis, virulence factors, antibiotic resistance, interaction with host, technology advances and emerging therapeutics. *Signal Transduct. Target. Ther.* **7**, 199 (2022).
34. Z. Pang, R. Raudonis, B. R. Glick, T.-J. Lin, Z. Cheng, Antibiotic resistance in *Pseudomonas aeruginosa*: Mechanisms and alternative therapeutic strategies. *Biotechnol. Adv.* **37**, 177–192 (2019).
35. L. B. Rice, Federal funding for the study of antimicrobial resistance in nosocomial pathogens: No ESKAPE. *J. Infect. Dis.* **197**, 1079–1081 (2008).
36. R. Van Twest, A. M. Kropinski, Bacteriophage enrichment from water and soil. *Methods Mol. Biol.* **501**, 15–21 (2009).
37. R. J. Grocock, P. M. Sharp, Synonymous codon usage in *Pseudomonas aeruginosa* PA01. *Gene* **289**, 131–139 (2002).
38. G. J. S. Lohman, "Selection of fusion-site overhang sets for high-fidelity and high-complexity Golden Gate assembly" in *Golden Gate Cloning: Methods and Protocols*, D. Schindler, Ed. (Springer US, US, New York, NY, 2025), pp. 41–60.
39. F. W. Studier, A. H. Rosenberg, Genetic and physical mapping of the late region of bacteriophage T7 DNA by use of cloned fragments of T7 DNA. *J. Mol. Biol.* **153**, 503–525 (1981).
40. C. K. Schmitt, I. J. Molineux, Expression of gene 1.2 and gene 10 of bacteriophage T7 is lethal to F plasmid-containing *Escherichia coli*. *J. Bacteriol.* **173**, 1536–1543 (1991).
41. A. Tabib-Salazar *et al.*, Full shut-off of *Escherichia coli* RNA-polymerase by T7 phage requires a small phage-encoded DNA-binding protein. *Nucleic Acids Res.* **45**, 7697–7707 (2017).
42. S. K. Zavriev, M. F. Shemyakin, RNA polymerase-dependent mechanism for the stepwise T7 phage DNA transport from the virion into *E. coli*. *Nucleic Acids Res.* **10**, 1635–1652 (1982).
43. R. Kiro, D. Shitrit, U. Qimron, Efficient engineering of a bacteriophage genome using the type I-E CRISPR-Cas system. *RNA Biol.* **11**, 42–44 (2014).
44. L. Cheng *et al.*, Harnessing stepping-stone hosts to engineer, select, and reboot synthetic bacteriophages in one pot. *Cell Rep. Methods* **2**, 100217 (2022).
45. A. Latka *et al.*, Engineering the modular receptor-binding proteins of *klebsiella* phages switches their capsule serotype specificity. *mBio* **12**, e00455-21 (2021).
46. K. Yehl *et al.*, Engineering phage host-range and suppressing bacterial resistance through phage tail fiber mutagenesis. *Cell* **179**, 459–469.e459 (2019).
47. M. Dunne *et al.*, Reprogramming bacteriophage host range through structure-guided design of chimeric receptor binding proteins. *Cell Rep.* **29**, 1336–1350.e1334 (2019).
48. M. Dunne, N. S. Prokhorov, M. J. Loessner, P. G. Leiman, Reprogramming bacteriophage host range: Design principles and strategies for engineering receptor binding proteins. *Curr. Opin. Biotechnol.* **68**, 272–281 (2021).
49. R. Lavigne *et al.*, The structural proteome of *Pseudomonas aeruginosa* bacteriophage phiKMV. *Microbiology (Reading)* **152**, 529–534 (2006).

50. D. P. Pires *et al.*, Pseudomonas phage vB_PaeP_P1G. National Center for Biotechnology Information. https://www.ncbi.nlm.nih.gov/nuccore/OQ230793.1. Accessed 20 December 2025.
51. P. J. Ceyssens *et al.*, Phenotypic and genotypic variations within a single bacteriophage species. *Virol. J.* **8**, 134 (2011).
52. E. Yirmiya *et al.*, Phages overcome bacterial immunity via diverse anti-defence proteins. *Nature* **625**, 352–359 (2024).
53. E. J. Slootweg *et al.*, Fluorescent T7 display phages obtained by translational frameshift. *Nucleic Acids Res.* **34**, e137 (2006).
54. A. Roberts, B. A. Adler, B. F. Cress, J. A. Doudna, R. Barrangou, Phage-based delivery of CRISPR-associated transposases for targeted bacterial editing. *Proc. Natl. Acad. Sci. U.S.A.* **122**, e2504853122 (2025).
55. B. G. Condron, J. F. Atkins, R. F. Gesteland, Frameshifting in gene 10 of bacteriophage T7. *J. Bacteriol.* **173**, 6998–7003 (1991).
56. L. Coppens, L. Wicke, R. Lavigne, SAPPHIRE.CNN: Implementation of dRNA-seq-driven, species-specific promoter prediction using convolutional neural networks. *Comput. Struct. Biotechnol. J.* **20**, 4969–4974 (2022).
57. A. P. Sikkema *et al.*, Pseudomonas phage 41S1. National Center for Biotechnology Information. https://www.ncbi.nlm.nih.gov/nuccore/PX380000.1. Deposited 17 September 2025.
58. S. Lund, V. Potapov, S. R. Johnson, J. Buss, N. A. Tanner, Highly parallelized construction of DNA from low-cost oligonucleotide mixtures using data-optimized assembly design and golden gate. *ACS Synth. Biol.* **13**, 745–751 (2024).
59. V. Zulkower, S. Rosser, D. N. A. Chisel, A versatile sequence optimizer. *Bioinformatics* **36**, 4508–4509 (2020).
60. K. Kortright *et al.*, A fully synthetic Golden Gate assembly system for engineering a Pseudomonas aeruginosa phiKMV-like phage [Dataset]. Dryad. https://doi.org/10.5061/dryad.pzgmsbd23. Deposited 4 December 2025.